https://doi.org/10.5194/egusphere-2025-506
Preprint. Discussion started: 4 April 2025

The impact of active and capable faults structural complexity on seismic hazard assessment for the design of linear infrastructures

Selina Bonini[1], Riccardo Asti[1], Giulio Viola[1], Giulia Tartaglia[2], Stefano Rodani[2], Gianluca Benedetti[2], Massimo Comedini[2], Gianluca Vignaroli[1]

[1]Department of Biological, Geological and Environmental Sciences, University of Bologna, Via Zamboni 67, 40126, Bologna, Italy
[2] ITALFERR S.p.A., Gruppo Ferrovie dello Stato Italiane – Architecture, Environment & Territory Department – Geology Division, Via Galati 87, 00155, Roma, Italy

Correspondence to: Selina Bonini (selina.bonini2@unibo.it)

Abstract. Since Active and Capable Faults (ACFs) may generate significant permanent deformation of the topographic surface, a careful evaluation of their spatial and geometric characteristics is essential for seismic hazard assessment when planning new linear infrastructures (e.g., roads, railway lines, pipelines). Although this is generally overlooked, the common structural complexity of fault zones leads to a non-uniform hazard along and across faults' traces, because of deformation localization and partitioning. This study reviews the factors controlling fault rupture and propagation, specifically focusing on fault zone architecture and growth mechanisms. Four scenarios of physical interaction between ACFs and linear infrastructures are analysed. The fault-crossing scenario is likely the most susceptible to ground surface displacement, while the fault-parallel scenario needs evaluation of the width of fault damage zone overlapping with the infrastructure. Near-fault tip and transfer zone-crossing scenarios require assessment of the local deformation patterns. The importance of a structural geological approach toward the reliable assessment of seismic hazard related to ACFs, we review suitable investigations to derive appropriate geological deterministic constraints on the geometry, kinematics, slip and deformation style of ACF's. Our approach may have significant impact on the legislation regulating the early stages of infrastructural design.

1 Introduction

The accurate definition of site-specific parameters and processes related to active faulting is becoming of increasing importance to seismic risk assessment. Although ground shaking is universally considered the primary cause of infrastructural damage, two large earthquakes in Alaska and Japan in 1964 (Mw = 9.2 and Mw = 7.4, respectively) have also highlighted the damaging potential of the effects of coseismic permanent ground deformation (Youd 2014), including ground surface rupturing by slip along active and capable faults (ACFs). An ACF is defined by the International Atomic Energy Agency (2010) as a fault capable of producing significant displacement at or near the ground surface in response to the activation of a seismogenic source at depth and that has moved within the framework of the current tectonic stress regime (the Late Pleistocene is taken as the lower time limit for interplate faults). The importance of including and quantifying infrastructure safety in the context of earthquake-related hazard has become evident after the 1906 San Francisco earthquake (Mw = 7.9, Prentice and Ponti 1997), when the Wrights tunnel recorded a 1.8 m offset along the trace of a ruptured seismogenic fault.

Fault rupturing is a complex phenomenon because of the common heterogeneity of the stress field acting along a fault zone, the variability of fault geometry and characteristics, the accumulated displacement history, and the lithological variability of the affected rocks (Ben-Zion and Sammis, 2003; Peacock et al., 2017; Treiman, 2010). In particular, the

https://doi.org/10.5194/egusphere-2025-506
Preprint. Discussion started: 4 April 2025

geometric and displacement attributes of a fault zone evolving through space and time are the direct expression of the mechanism(s) and the tectonic context controlling fault nucleation and progressive growth (Cartwright et al., 1995; Fossen and Rotevatn, 2016; Morley et al., 1990). If the fault is seismically active, these parameters also depend on earthquake magnitude, and they relate to it as predicted by empirical scaling relationships (Ferrill et al., 2008; Kim and Sanderson, 2005; Leonard, 2010; Schultz et al., 2008; Vermilye and Scholz, 1998; Walsh et al., 2002; Wells and Coppersmith, 1994). Until now, conventional approaches aimed at assessing seismic hazard in a given area have unfortunately overlooked both the structural and geometrical complexities of active fault zones as well as the cross-cutting relationship between variably oriented faults and/or fault segments within bigger and more complex fault zones. Furthermore, distinct modes of deformation accommodation (i.e., rupturing along a single discrete slip surfaces or by diffuse off-fault deformation affecting a wider volume of rock) can lead to different patterns of permanent deformation at the ground surface, as evidenced by probabilistic fault displacement hazard analysis scenarios of ACFs (e.g. Moss and Ross, 2011; Petersen et al., 2011; Youngs et al., 2003).

The geohazard associated with the occurrence of ACFs in seismotectonically active areas is of particular interest to the design and construction of linear infrastructures (such as roads, railways, gas/oil pipelines, and power lines) that, unlike punctual infrastructures (such as buildings, dams or nuclear installations), may extend over even hundreds of kilometres, thus potentially interacting with multiple tectonic features that possibly belong to very different tectonic contexts. Researchers engaging with this applied issue worldwide carry out seismic risk assessment primarily from an engineering and geotechnical perspective, thus dominantly focusing on the exposure or vulnerability of existing infrastructure networks (Shinoda et al., 2022; Zhu et al., 2020). There is, instead, a remarkable knowledge and legislative gap regarding the hazard due to ACFs in the case of new linear infrastructures that run across a seismically active region. An approach based on fault scaling laws has been recently proposed to estimate fault displacement hazard at lifelines-fault interference sites (e.g. Melissianos et al., 2023). That method, however, does not account for the complexity of fault characteristics and their temporal and spatial variability.

Numerous scientific studies have been conducted around the world to learn more on ACFs. This constantly refined knowledge is being used to populate open-access databases that are fundamental to seismic hazard assessment (e.g. https://dggs.alaska.gov/pubs/id/24956; https://gbank.gsj.jp/activefault/index_e.html; https://data.gns.cri.nz/af/). The potential impact of seismic fault-related effects should be distinguished based on how ACFs geometrically interact and physically interfere with a linear infrastructure. Thus, a careful and quantitative analysis of the relationships between ACFs and linear infrastructures should be carried out already during early feasibility studies, as a support for the later engineering infrastructure design phase.

In this study, we analyse four possible geometrical interference situations between ACFs and linear infrastructures: fault-crossing, fault-parallel, near-fault tip, and transfer zone-crossing scenarios. For each case, we establish a) the main fault structural features to be defined and investigated, b) the related key fault parameters to be assessed and c) the most suitable investigations to use to derive appropriate geological deterministic constraints on geometry, kinematics, slip and deformation style of the ACF. By using as an example the national reference database for Italian ACFs (ITHACA Working Group, 2019; Errore. L'origine riferimento non è stata trovata.) and relevant seismic microzonation legislations (Technical Commission on Seismic Microzonation, 2015), we propose an operative workflow to comprehensively parametrise an evolving ACF. This study can inform ever more realistic scenarios of probabilistic fault displacement hazard analysis and, ultimately, aid in developing mitigation strategies to minimize infrastructure vulnerability.

https://doi.org/10.5194/egusphere-2025-506
Preprint. Discussion started: 4 April 2025

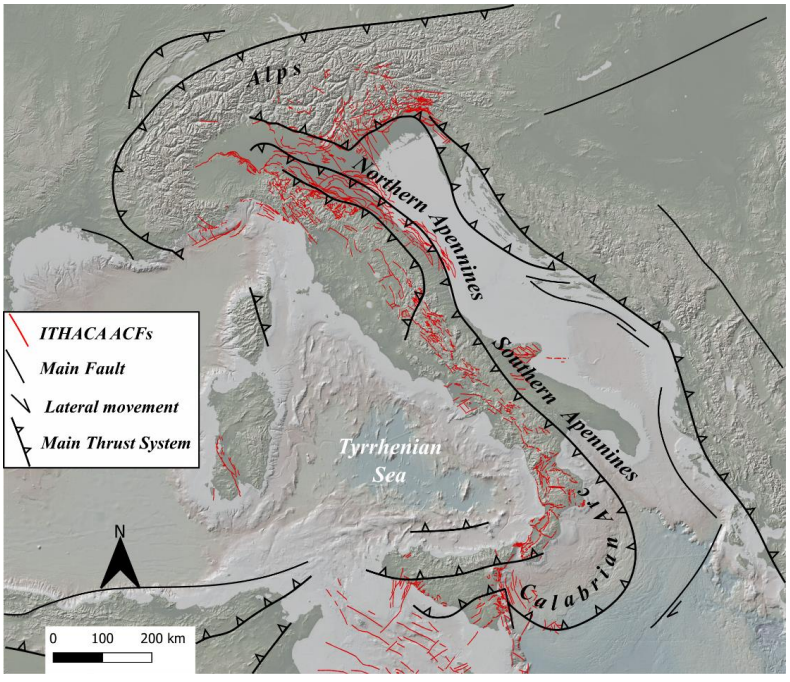

Figure 1: ACFs as per the ITHACA Italian catalogue (ITHACA (ITaly HAzard from CApable faulting), A database of active capable faults of the Italian territory, 2024) framed within the tectonic setting of Italy.

2 Factors controlling fault rupturing and rupture propagation at the surface

Surface faulting is commonly associated with earthquakes with Mw ≥ 6, although the 2018 Lake Muir (Australia, Mw = 5.3, Clark et al., 2020) and 2019 Le Teil (France, Mw = 4.9, Ritz et al., 2020) moderate seismic events have also ruptured the ground surface. Recently, a database has been compiled listing surface rupturing data from 50 historical and instrumental earthquakes between 1872 and 2019 from all over the world (SURE 2.0, Nurminen et al., 2022). This database clearly shows that several factors steer the propagation of coseismic ruptures to the ground surface. In this regard, "external" and "internal" factors can be distinguished with respect to the fault system. External factors include the system characteristics that directly relate to the host rock and fluids. Rock rheology, for instance, is usually recognised as a controlling factor of rupture propagation, as narrow fault zones of high shear strain are typically associated with quartz-feldspathic rock types, whereas wide zones with diffuse high shear strain are commonly located in phyllosilicate-rich protoliths (Chester and Logan, 1986; Faulkner et al., 2003, 2008). Fault rupturing is facilitated during fluid-assisted deformation, as pore pressure reduces the normal stress on locked faults. Viscosity contrasts and the overburden thickness, in addition, control shear localization, which varies markedly passing from the bedrock to unconsolidated and/or water saturated sediments (Bray et al., 1994; Irvine and Hill, 1993; Johnson et al., 1997; Lazarte et al., 1994; Reid, 1910; Tchalenko, 1970).

Internal factors, on the contrary, represent all fault parameters that are connected with its kinematics, geometry, and mechanics. Fault orientation is known to exert significant impact on the kinematics of a given fault (Bott, 1959; Wallace, 1951), and numerous studies have shown that off-fault coseismic deformation is more likely localized in the hanging wall of inclined faults (Axen et al., 1999; Fletcher and Spelz, 2009; Huang and Johnson, 2010; Ma, 2009). Consequently, the kinematic characteristics of a fault affect the width of the surface rupture zone: a fault with pure strike-slip or pure dip-

https://doi.org/10.5194/egusphere-2025-506
Preprint. Discussion started: 4 April 2025

slip movement is generally narrower than oblique slip faults. Other factors to consider are the coseismic slip magnitude and slip kinematics (Bray et al., 1994; Horsfield, 1977; Naylor et al., 1986; Quigley et al., 2012; Schlische et al., 2002; Tchalenko, 1970). In tectonically active areas, in fact, geometric parameters of a fault, such as coseismic length rupture and displacement recorded at the ground surface, are directly related to the moment magnitude of the earthquakes generated by it, as demonstrated by scale relationships (e.g. Wells and Coppersmith, 1994; Leonard, 2010). Figure 2 shows well-known databases of coseismic surface ruptures events integrated with data documented during historical and instrumental strong earthquakes (Table 1). Coseismic fault data (including maximum displacement and rupture length at the ground surface) exhibit a three-order-of-magnitude variation (from centimetres to tens of meters) for earthquake events ranging from magnitude 5 to 9 Figure 2a,b). This variation applies to all fault types (normal, reverse, and strike-slip) and can be attributed to factors influencing the propagation of fault rupture towards the topographic surface, along with the specific growth mechanisms governing each fault system (see below).

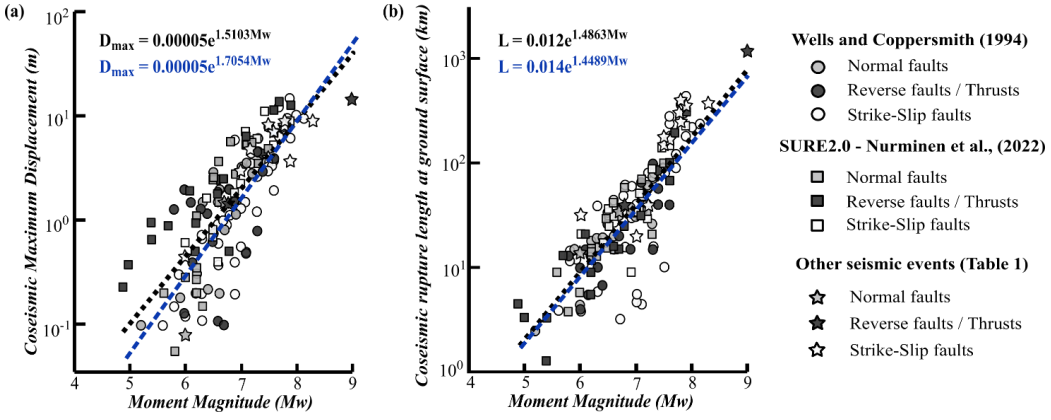

Figure 2: Scaling laws correlating coseismic geometric fault attributes (maximum displacement and rupture length at the ground surface) and earthquake magnitude (a, b, respectively). Blue trend lines are calculated from Wells and Coppersmith (1994), black trend lines are calculated considering also data from the SURE2.0 database (Nurminen et al., 2022) and Table 1.

Table 1: Historical and instrumental earthquakes that produced coseismic displacement at the ground surface and that are not included in Wells and Coppersmith (1994) and SURE2.0 (Nurminen et al., 2022) datasets. L: length; Dmax: maximum displacement.

Location		Year	Mw	L (km)	D_{max} (m)	Kinematics	References
USA, CA	Parkfield	2004	6	32	0.46	Strike-Slip	Lienkaemper et al. (2006)
Turkey	Düzce	1999	7.2	40	5		Wesnousky (2008)
China	Kokoxili	2001	7.8	400	8		Lasserre et al. (2005)
Mongolia	Bolnai	1905	8.3	375	9		
Turkey	Erzincan	1939	7.9	350	3.7		
China	Dongxi Co	1930	7.5	150	4		Klinger et al. (2005)
	Manyi	1997	7.6	170	7		
Turkey	Pazarcik	2023	7.8	300	7.76		Dai et al. (2024)
	Elbistan	2023	7.5	180	8.2		
Indonesia	Sumatra	2004	9	1200	15	Reverse	Fujii et al. (2021)
Armenia	Spitak	1988	6.8	40	1.6	Reverse-Oblique	Philip et al. (1992)
Italy	Avezzano	1915	6.7	35	1.2	Normal	Galadini and Galli (1999)
	Colfiorito	1997	6	14	0.08		Cello et al. (2000)

https://doi.org/10.5194/egusphere-2025-506
Preprint. Discussion started: 4 April 2025

3 Fault zone architecture and growth mechanisms

3.1 Fault zone architecture and attributes

Commonly, the first-order architecture of a fault zone (Figure 3) includes a central core and enveloping damage zones (e.g. Caine et al., 1996; Cello et al., 2000; Chester et al., 1993; Chester and Logan, 1987). The fault core represents the product of highly localized deformation and most of the displacement within the faulted volume is accommodated therein (e.g. Bruhn et al., 1994; Childs et al., 1996; Sibson, 1977), as it is composed of multiple slip surfaces and fault rocks, such as fault gouge, breccia, and lenses of host rock (Torabi et al., 2019). Damage zones, instead, are characterised by relatively low deformation compared to fault cores. These zones generally exhibit several second-order structures such as subsidiary faults, fractures, veins, stylolites, cleavage, fault-related folds and/or drag folds (e.g. Berg and Skar, 2005; Billi et al., 2003; Bruhn et al., 1994; Faulkner et al., 2010; Odling et al., 2004).

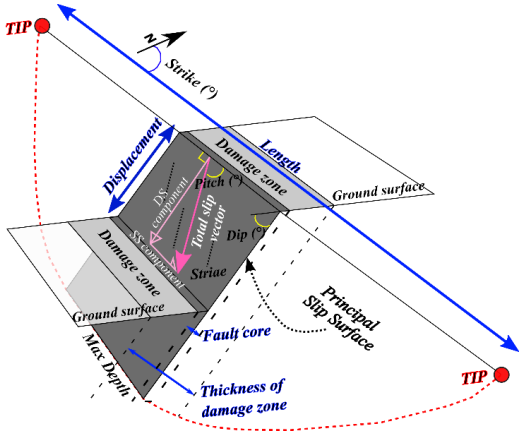

Figure 3: Schematic illustration of a fault zone and definition of its main attributes.

The thickness (or width, in map view) of these two structural domains, their strike and dip angles, length, maximum depth, and displacement represent the geometric attributes of a fault that need to be constrained when building the fault source model in seismic hazard analysis. However, the intricate nature of fault zones can lead to significant variability in fault parameters both along and across the fault zone (Figure 4), suggesting that variable mechanisms of nucleation and growth may contribute to fault zone evolution in space and time. This variability may thus have a substantial impact on the resolution and reliability of seismic hazard estimates.

https://doi.org/10.5194/egusphere-2025-506
Preprint. Discussion started: 4 April 2025

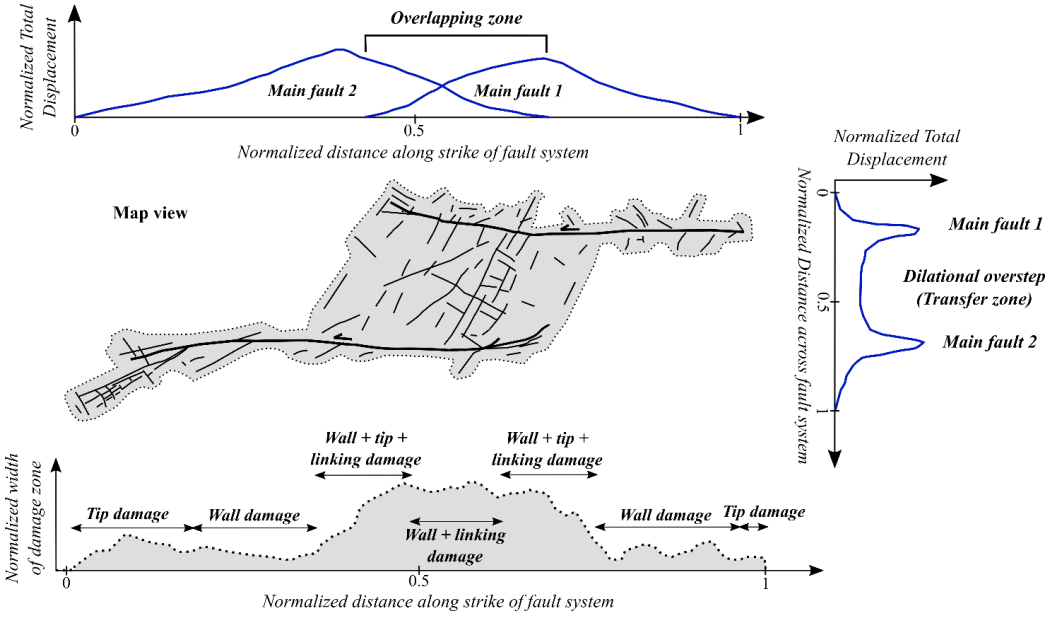

Figure 4: Variable along- and across-strike displacement distribution and width of a complex fault zone.

Fault core geometry, for instance, varies in response to how deformation is localized in the rock volume, which is a function of the geomechanical properties of the host rock, the competency contrasts of the faulted lithotypes and of the presence of pre-existing anisotropies (e.g. Bastesen and Braathen, 2010; Childs et al., 2009; Foxford et al., 1998; Shipton et al., 2005, 2006; Sperrevik et al., 2002; van der Zee and Urai, 2005; Wibberley et al., 2008). In general, average values of fault core thickness vary between millimetres to one meter for an average (cumulative) displacement ranging from some centimetres to a few tens of meters (Johannessen, 2017; Torabi et al., 2019; Figure 5a). However, exceptional cases with fault displacements exceeding hundreds of kilometres have cores up to ten-hundreds of meters thick as well (e.g. Childs et al., 2009; Wibberley et al., 2008).

Damage zones, on the other hand, include thicker rock volumes. Their width is usually defined by the frequency distribution of damage structures that commonly decreases with distance from the fault core (e.g. Chester and Logan, 1987; Goddard and Evans, 1995; Scholz, 1994; Smith et al., 1990). Many authors have related it to the cumulative displacement (e.g. Faulkner et al., 2011; Fossen et al., 2007; Torabi et al., 2020; Torabi and Berg, 2011; Figure 5b) or to the fault length (Vermilye and Scholz 1998 and references therein, in terms of process zone, Figure 5c). Scaling laws reveal that the width of a damage zone can vary from centimetres to kilometres for cumulative displacements varying within a similar range. Scattered data suggest that the width of the damage zone is typically two orders of magnitude smaller than the fault length.

https://doi.org/10.5194/egusphere-2025-506
Preprint. Discussion started: 4 April 2025

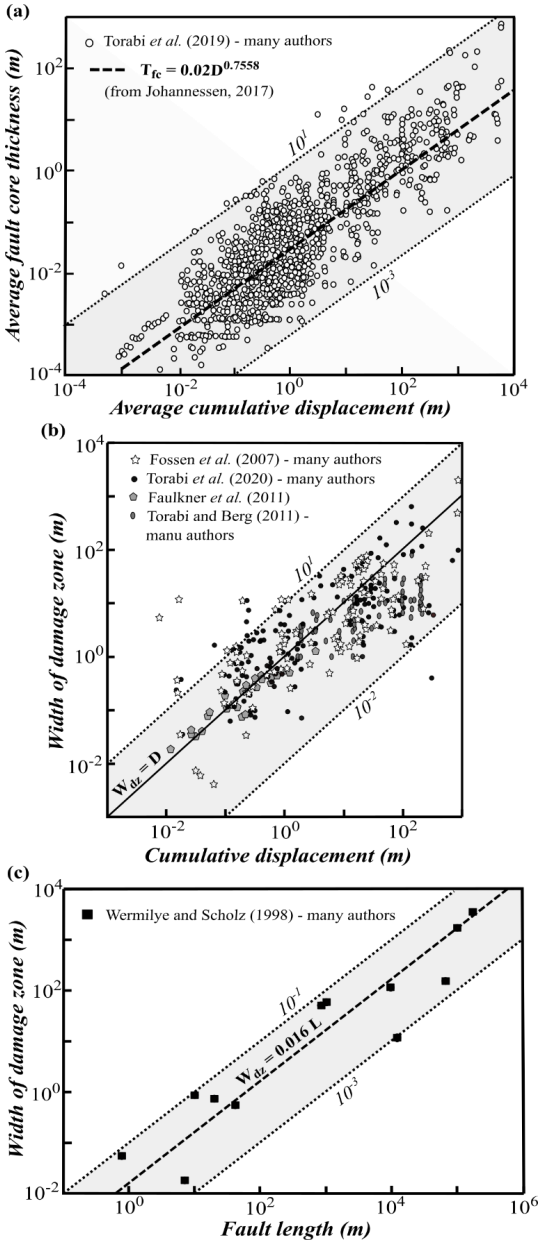

Figure 5: (a) Fault core average thickness vs. average (cumulative) displacement (power-law relationship from Johannessen 2017; data after Torabi et al. 2019 and references therein). (b) Scaling law between fault damage zone width (data after Fossen et al. 2007 and references therein; Faulkner et al. 2011; Torabi and Berg 2011 and references therein; Torabi et al. 2020 and references therein); (c) Scaling law between cumulative offset and fault length (data after Vermilye and Scholz 1998 and references therein). Dotted lines are evaluated from y = x.

Damage zones are variably named depending on their location within and around the fault (*wall* vs *tip* damage zone), or between fault segments (*linking* damage zone) (Figure 4; Kim et al., 2004). A damage zone can become much wider

https://doi.org/10.5194/egusphere-2025-506
Preprint. Discussion started: 4 April 2025

during fault interaction and may also include the tip damage zone, which usually contains structures that are misoriented to the main fault surface and that can accommodate shear movement or just tension opening (Kim et al., 2004, 2000, 2003; Kim and Sanderson, 2006; McGrath and Davison, 1995). For steeply dipping faults, subsidence and formation of fault propagation folds may cause the propagation of secondary structures preferably in the hanging wall (Berg and Skar, 2005; Evans, 1990; Ferrill et al., 2005), resulting in an uneven damage zone across the fault strike. Berg and Skar (2005) suggest a further subdivision of the fault damage zone in hanging wall and footwall damage zones, due to structural and geometric differences of secondary slip surfaces and fractures.

Fault displacement profiles, then, are controlled by several factors, including fault length (in map view), the fault aspect ratio (i.e., the ratio between fault length and height), fault shape (rectangular vs. elliptical), proximity of the fault to the free surface or other boundaries, configuration of far-field stresses, frictional and constitutive properties of the fault, variations in elastic properties and lithology along the fault, time-dependent rheology, near-tip processes, interaction with other faults, and fault segments linkage (e.g. Peacock, 2002; Schultz, 1999). Typically, displacement is considered zero at the fault tips and increases up to a maximum near the centre of the fault (Barnett et al., 1987). In the case of hard-linked fault segments, however, Peacock and Sanderson (1991, 1994) noted that the displacement gradient of a fault increases in the zone where fault segments overlap, and that the displacement maximum is no longer in the centre but located closer to the overlap zone (Figure 4).

Other fundamental fault attributes that have a relevant impact on seismic hazard assessments are fault kinematics (slip vectors and sense of shear), and state of activity (slip rate, recurrence interval for surface faulting, slip – total and per event – and triggering related earthquakes). Their estimation is necessary to fully parametrize a complex fault zone.

3.2 Fault nucleation and growth mechanisms

Following initial nucleation, the growth of a single fault can be ascribed to two main mechanisms (Figure 6): i) tip propagation and ii) displacement accumulation without significant tip propagation. Both growth processes refer to the development of a single, isolated fault.

In the case of the tip propagation model, faults form by developing a process zone, where micro-fractures form and coalesce along strike of the growing fault (Cowie and Shipton, 1998). Cox and Scholz (1988) demonstrated that Mode III shear cracks generate and link ahead of the crack tip. This leads to an increase in displacement proportional to the growth of fault length (e.g. “constant Dmax/L ratio model”), with maximum displacement values at the centre of the fault. Further fault evolution is accomplished by stress concentration at the tips, implying the development of various deformation features at the fault terminations, including wing cracks, horsetail fractures, fan-shaped branch faults, en échelon synthetic or antithetic shear fractures (Kim et al., 2004, 2000).

The second fault evolution mechanism leads to rapid growth and subsequent displacement accumulation without significant tip propagation (“Constant length model”, Walsh et al., 2003). It is mainly applied to the development of a long fault structure above a buried reactivated fault (e.g. Giba et al., 2012). Slip in this case imposes an extension with deformation localizing in the cover above the fault, and overall fault propagation is upwards from the reactivated fault, generating tip bifurcation. It implies significant widening of the (wall-) damage zone.

When two subparallel, separated fault segments approach, they start to interact (e.g. Trudgill and Cartwright, 1994; Walsh et al., 2003). This is manifested by the curving of their terminations, bifurcation, development of a complex zone of subsidiary structures (splays, faults, fractures, deformation bands) or the formation of relay ramps (Fossen and Rotevatn, 2016). The interaction potentially evolves through time in linkage (“Fault linkage model” within fault population), causing extensional or contractional oversteps (Kim et al., 2004). In this regard, Peacock et al. (2017) made a distinction between

https://doi.org/10.5194/egusphere-2025-506
Preprint. Discussion started: 4 April 2025

i) approaching damage zones, if the interacting faults are kinematically linked but do not intersect, and ii) intersecting damage zones, which form around the intersection between two or more faults that abut, splay, or crosscut coevally (formed under the same tectonic regime) or sequentially (formed under different tectonic regimes). This second sub-category also includes the linking damage zone described by Kim et al. (2004) as regarding the area of deformation at a step between two sub-parallel coeval faults. When deformation is transferred from a fault to another, the intervening deformation area is called transfer zone. Morley et al. (1990) introduced a systematic classification scheme for transfer zones, based on the dip direction (divergent or convergent) and the degree of overlap of faults between which the displacement transfer occurs. In transfer zones, deformation is distributed over a wider rock volume through diffuse faulting. The variable displacement transfer between shear structures and real fault zone depends on the overlap degree between two faults or fault segments. The interaction between faults is also related to the spacing and the total length of the fault systems, depending on their kinematics. For example, laboratory experiments document that strike-slip faults interact when the spacing between two main faults is less than 10% of the combined fault length (An, 1997), while field data have been used to infer that normal fault systems interact when the ratio between their minimum length and spacing is >14 (Acocella et al., 2000).

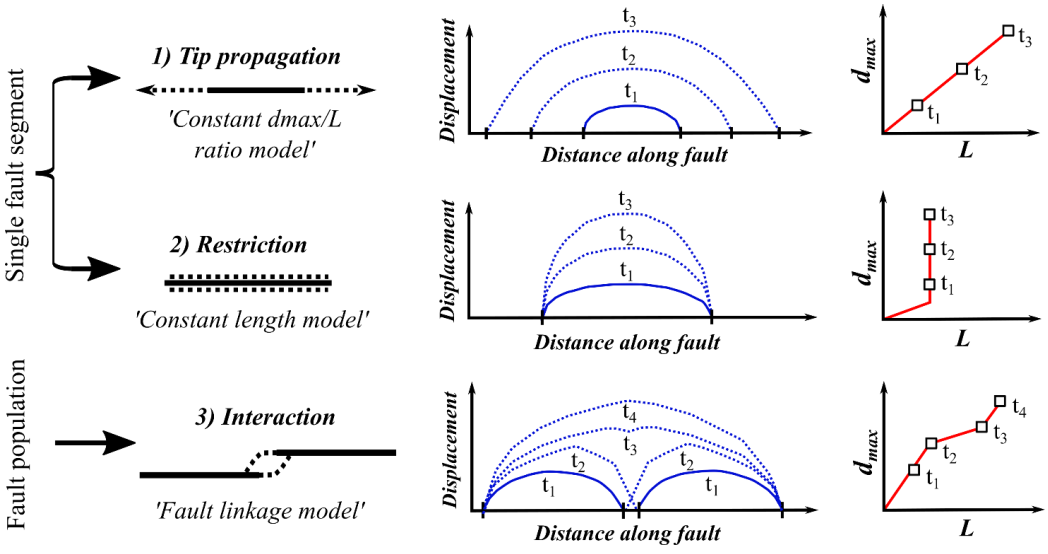

Figure 6: Possible nucleation and growth mechanisms of faults. t_1-t_4 are sequential time increments during which a fault evolves.

4 Geometric interference patterns between ACFs and linear infrastructures

In this section, we apply the fault attributes and growth mechanisms described above to an ideal scenario of ACF evolution. Firstly, we analyse the impact of these mechanisms upon the four most likely geometric interference patterns between an ACF and a linear infrastructure. Then, we define a spectrum of structural geological parameters that should be carefully monitored at the interference zones (IZ) between an ACF and the linear infrastructure (Table 2). We define the IZ as the mappable area where the deformation effects associated with ACFs activity are expected to impact the infrastructure.

https://doi.org/10.5194/egusphere-2025-506
Preprint. Discussion started: 4 April 2025

We have considered the following fault-linear infrastructure interference patterns (Figure 7): i) *Fault-crossing infrastructure*, if the linear infrastructure intersects the trace of a main fault at any incidence angle along its length; ii) *Fault-parallel infrastructure*, if the linear infrastructure runs essentially parallel to the main fault trace, potentially interfering with the ACF damage zone and/or its core; iii) *Near-fault tip infrastructure*, if the linear infrastructure runs at or near the influence lobes characterizing the ACF tip points; iv) *Transfer zone-crossing infrastructure*, if the linear infrastructure passes by an area located between two or more interacting ACFs or ACF segments.

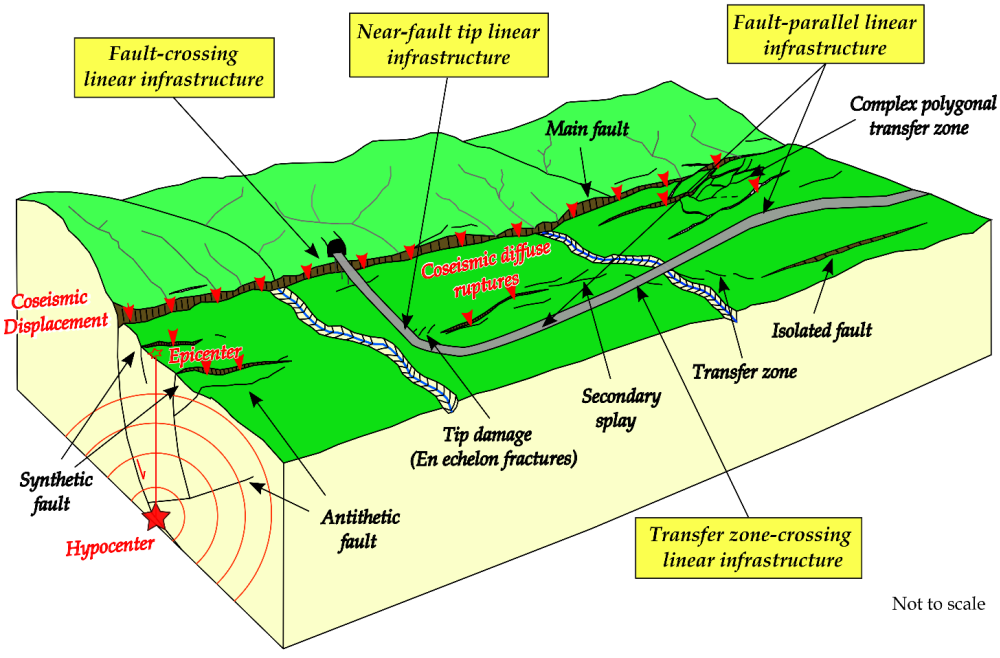

Figure 7: Schematic diagram illustrating possible geometrical interference patterns between an ACF and a linear infrastructure.

Since the crossing of different portions of an ACF by a linear infrastructure implies that some fault parameters may weigh more than others, each scenario requires a distinct assessment of the fault parameters associated with the corresponding ACF element. Thus, we can prioritize some fault parameters over others in fault hazard assessment (Figure 8).

https://doi.org/10.5194/egusphere-2025-506
Preprint. Discussion started: 4 April 2025

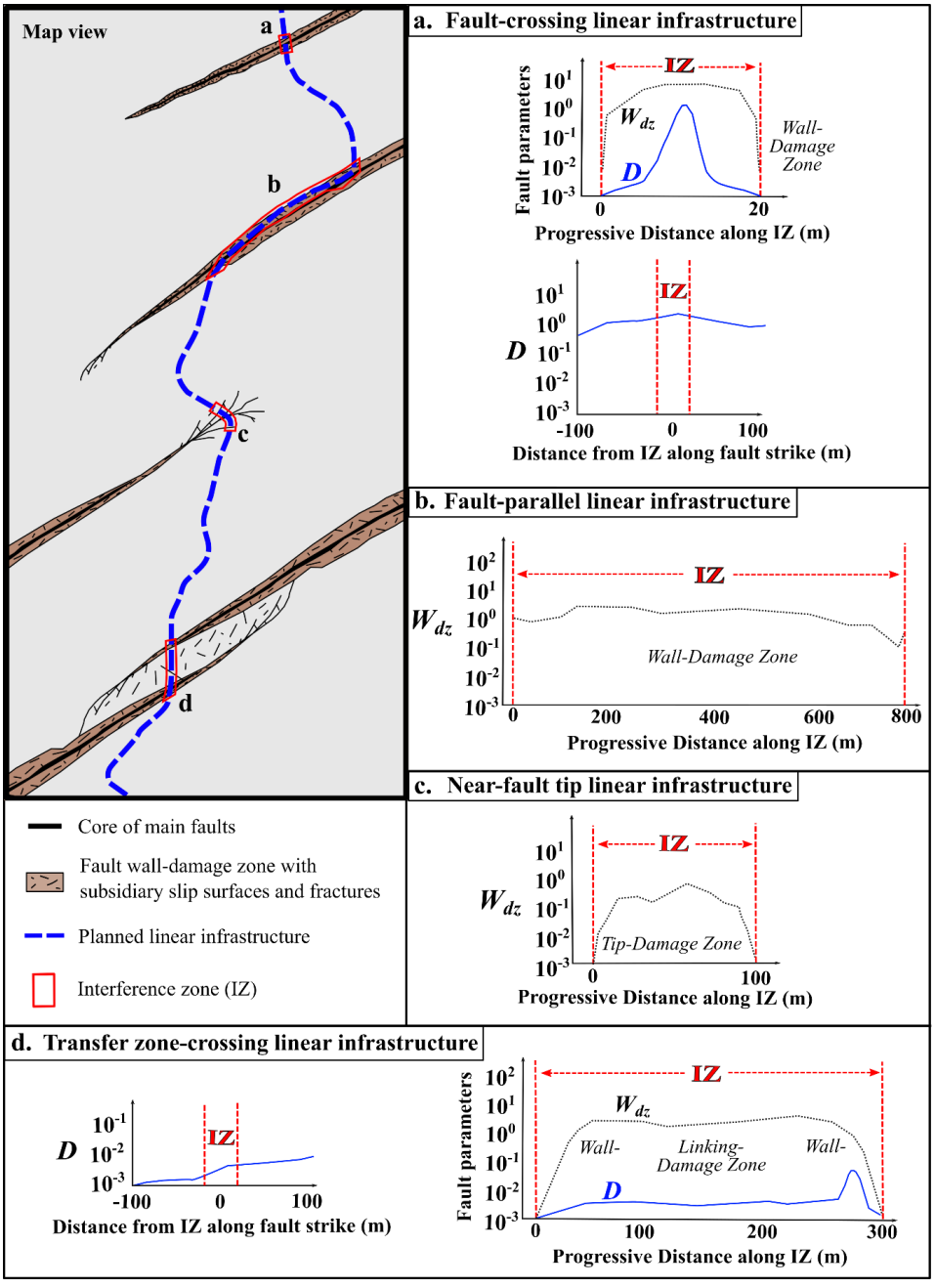

245 **Figure 8: Examples of potentially useful parameters for defining the discussed four fault-linear infrastructure interference scenarios (D = displacement, Wdz = width of damage zone, in graphs a-d). Drawing not to scale.**

In a *fault-crossing* scenario it is particularly important to investigate (i) the coseismic displacement at the ground surface, especially if the offset is accommodated through narrow slip surfaces, and (ii) the deformation accommodated within the damage zone. (i) While in fault source models a unique mean value of slip is usually considered for the entire ACF,

https://doi.org/10.5194/egusphere-2025-506
Preprint. Discussion started: 4 April 2025

displacement is variable along the strike of a fault (e.g. Peacock, 2002; Schultz, 1999); Figure 4). Both fault growth mechanisms (single fault segment and fault population; Figure 6) predict that the maximum displacement is expected to occur at the centre of the fault system, while it gradually decreases to zero at the fault tips. (ii) Based on scaling relationships (Figure 5b), the width of the damage zone linearly correlates with cumulative displacement. Thus, the maximum width of the damage zone is expected to coincide with the zone of maximum displacement at the centre of the fault system. From the consideration above, it is reasonable to expect that the potential impact linked to coseismic displacement and damage zone development can be higher if the linear infrastructure crosses the central zone of a fault system (either fault segment or interacting fault segments), rather than near the tips. To obtain high-resolution data on both amount of displacement and damage zone width at the IZ, it is crucial to analyse the distribution of deformation both along fault strike (for displacement) and across the fault strike (for damage zones; Figure 8a).

The extent of the study area on both sides of the linear infrastructure should be calculated considering the scaling relationships in Figure 2a,b, and Figure 5c. During design stage, the area usually included in the detailed study extends for few hundreds of meters away from the linear infrastructure, on both sides. For example, this extent is probably more than sufficient in the case of the Italian territory. In fact, coseismic deformation is expected to affect an area of maximum tens of meters, with the occurrence Mw = 7 earthquakes, which is, at the moment, the highest magnitude value reported in the historical seismological record of Italy. However, this distance from the infrastructure might be inadequate in the case of stronger earthquakes.

In a *fault-parallel* scenario, it is critical to verify if the infrastructure interacts with the fault damage zone (Figure 8b) and, eventually, to evaluate the length of the infrastructure section falling within the IZ. Similar to the previous scenario, constraining the width of the damage zone requires considering the position of the IZ relative to the length of the main slip surface (central part or toward the tips). Scaling laws suggest that the width of the damage zone is c. a couple of orders of magnitude lower than fault length (Figure 5c) and thicker in the hanging wall of dipping faults.

In a *near-fault tip* scenario, the deformation associated with fault tips is particularly significant. Deformation structures at the IZ stem from how the fault accommodated displacement at its tips as it progressively grew in length over time (fault growth mechanism by tip propagation in Figure 6). It is, hence, a priority to evaluate the extent of the area that is affected by fractures (tip damage zone), including its potential further growth during future earthquakes (Figure 8c). For high angle and steeply dipping faults, the assessment of deformation near the fault tips becomes even more critical, as the tips of these faults can be associated with a broad range of fracture patterns, depending on the fracturing propagation mode and the deviatoric stress existing at the tips (Kim et al., 2004, 2000, 2003; Kim and Sanderson, 2006; McGrath and Davison, 1995).

The *transfer zone-crossing* scenario implies the interaction between two (or more) active faults where deformation is accommodated both along each single fault segment as well as in the fault overstep region. This complex structural setting encompasses all fault mechanisms and variations of fault characteristics described previously. In this scenario, the complexity of the IZ is linked to the width of the damage zone that develops during fault interaction (Figure 4). It is necessary to consider both the extent of the zone affected by diffuse deformation within the damage zone (wall damage zone plus linking damage zone) and the fact that there are discrete surfaces potentially accommodating most of the displacement. The priority should be the quantification of both the width of the transfer zone-related damage zone crossed by the linear infrastructure and the slip accommodated by the main fault surfaces (if crossed; Figure 8d). During planning, in fact, it is essential to recognize whether the estimated coseismic displacement will be accommodated by fault zones a few meters thick, rather than by secondary planes within an extensive damage zone of hundreds of meters. Therefore, the same considerations made for the assessment of the displacement are applied. Transfer zones can moreover exhibit

https://doi.org/10.5194/egusphere-2025-506
Preprint. Discussion started: 4 April 2025

complex arrays of synthetic and antithetic shear fractures, which can define blocks that can potentially rotate during coseismic rupturing (Kim et al., 2000) . If these blocks have a considerable dimension with respect to the linear infrastructure, the probability of rotation during ACF activation should be also included in the fault hazard assessment.

5 Discussion

5.1 ACF parameters characterization

To date, neither scientific studies nor international guidelines (e.g. International Atomic Energy Agency, 2010) have proposed a procedure to assess and characterize the structural complexity of ACFs as a support to seismic hazard assessment in infrastructural design. In Italy, existing guidelines for seismic microzonation studies (Technical Commission on Seismic Microzonation, 2015) prescribe the mapping of ACFs with the aim to outline respect areas in map view linked to the kinematics of the fault (ratio footwall/hanging wall = 1:4 for normal faults; 1:2 for reverse faults). However, nothing specific is suggested/recommended concerning the characterization of ACFs and the variation of their parameters in space.

Since ACF behaviour and attributes are strictly connected to the mechanisms by which the fault has developed, we propose an approach to optimize hazard assessment according to fault structural complexities and fault-linear infrastructure interference patterns. The assessment of seismic hazard due to the occurrence of ACF(s) should, therefore, address the study of specific fault attributes for each of the considered interference scenarios. This can be useful in a very preliminary phase of the design stage such as the feasibility study, especially for linear infrastructures of considerable length intersecting several potential ACFs.

Our study shows that:

- Coseismic displacement and damage zone width are crucial fault parameters, which are strictly linked to the structural architecture of an ACF. The variability observed in these fault parameters is related to the growth mechanism considered for the ACF.
- How an ACF geometrically interacts and physically interferes with a linear infrastructure defines distinct potential types of influence on the seismic fault-related effects. This emphasizes the importance of considering these pattern interactions and prioritizing the characterization of key fault aspects for the four scenarios presented above. Figure 9 proposes a summary of the main priority for assessing specific ACF parameters for each scenario.
- The incidence angle between the linear infrastructure and the ACF is a critical factor (Figure 10). The zone potentially impacted by fault deformation tends to be larger when the linear infrastructure crosses the ACF at lower angles. Conversely, a nearly perpendicular intersection (high angle) may result in a relatively small IZ; on the other hands, the IZ may involve the entire infrastructural segment of interest if the infrastructure runs parallel to the ACF and lies within the damage zone.
- The parametrization of the fault-linear infrastructure interference patterns could be considered as independent from the kinematics of the fault itself.

If the full parametrization of ACFs cannot be performed due to the inaccessibility of the site or the low quality of outcrops, it is possible to use fault scaling laws (Figure 2a,b) to predict the expected range of deformation along an ACF for a given maximum earthquake magnitude (e.g. Leonard, 2010; Wells and Coppersmith, 1994). It could be, at a first approximation, an indicator of the magnitude of the expected coseismic deformation at the ground surface that could involve the infrastructure.

https://doi.org/10.5194/egusphere-2025-506
Preprint. Discussion started: 4 April 2025

The parameterization of the geometric properties of the fault zone in *Figure 5a,b,c* provides the extend of the area in which the coseismic rupture associated with a given magnitude can localized, leading to the development of distributed ruptures.

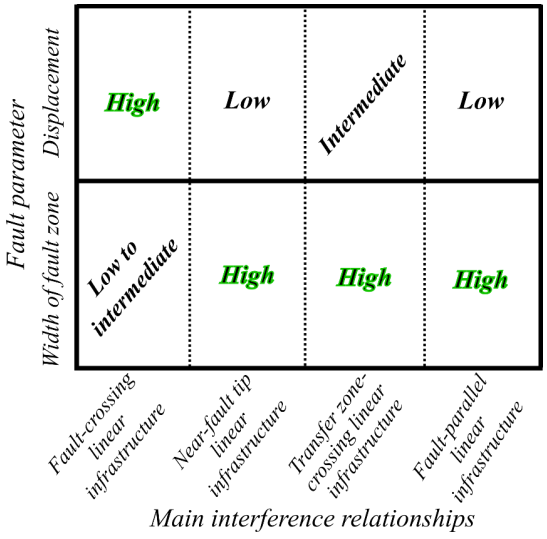

Figure 9: Schematic correlation between fault parameters and fault-linear infrastructure interference pattern. For each scenario, the recommended priority for assessing specific ACF parameters is qualitatively indicated.

https://doi.org/10.5194/egusphere-2025-506
Preprint. Discussion started: 4 April 2025

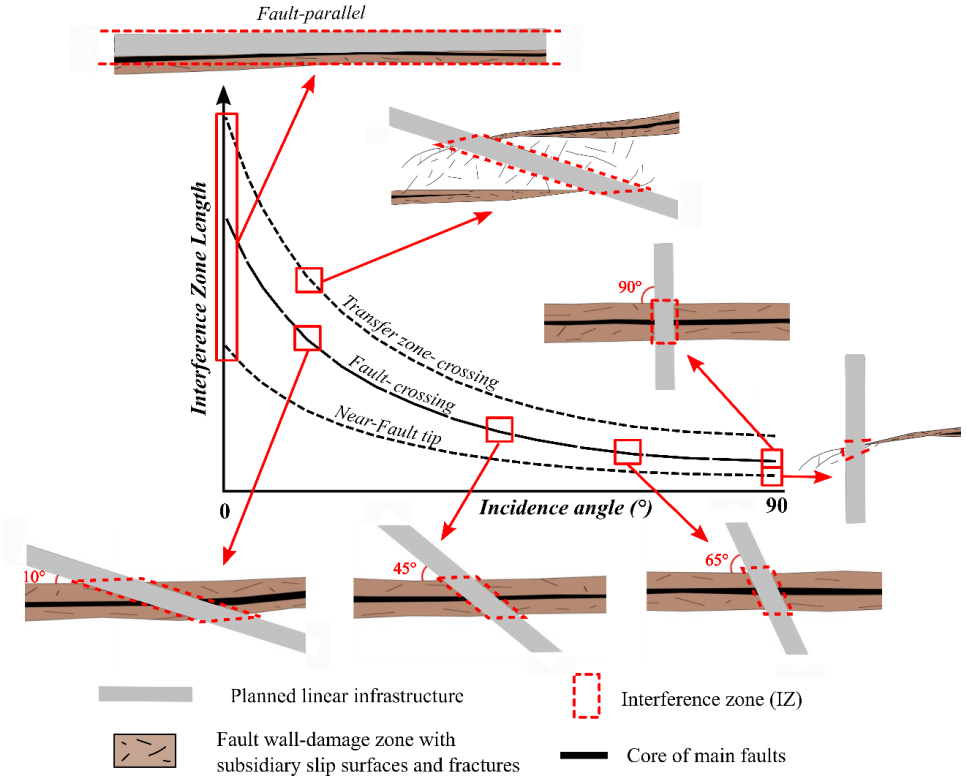

Figure 10: Variation of the area potentially affected by ACF effects (dotted red area) as a function of the incidence angle and the ACF-linear infrastructure scenario.

5.2 Toward a structural-based approach for the Seismic Hazard Assessment in Linear Infrastructure design

In order to characterize the style and mechanisms governing the structural complexity of an ACF at fault-linear infrastructure interference zones, we propose a structural geological approach that is to be implemented during the design phase of an infrastructure project (Table 2). This approach supports a multidisciplinary and multiscalar work that integrates traditional methods (e.g. aerophotogrammetry, paleoseismology) and new developments (e.g. Remote Sensing analysis, geophysical investigations) for the characterization of areas affected by active tectonics (McCalpin, 2009, 2013). These methods may estimate slip rates over different time scales (Cowie and Roberts, 2001) such that we should carefully consider which is the best method to be used for a specific scenario of seismic hazard assessment. It is noteworthy that a geological and structural study of the site of interest is a fundamental step, that permits to collect quantitative structural data and ground-truth all the data collected by indirect techniques.

Once the presence of a potential ACF has been ascertained (for example, by relying on dataset of ITHACA and/or seismological databases, seismic microzonation studies, fieldwork evidence, geological cartography, and/or scientific literature), detailed investigations should be started at a smaller scale, aiming to evaluate the geometric ACF-linear infrastructure interference scenario and what portion of the ACF can potentially involve the planned linear infrastructure. This evaluation represents the starting point of a structural geology-based seismic hazard assessment. The suggested operative workflow can be enriched with a morpho-tectonic study performed with remote sensing data. Remote sensing

https://doi.org/10.5194/egusphere-2025-506
Preprint. Discussion started: 4 April 2025

is a useful indirect method to perform morpho-structural analyses over large areas. It can rely on the analysis of digital terrain models (DTMs) or LiDAR (Light-Detection and Ranging; laser scanning) data, the latter being capable of reproducing DTMs by filtering the vegetation cover. High resolution LiDAR images can be used to evaluate fault zone width, by identifying off-fault deformation features, rupture complexity, and post-seismic phenomena (Nissen et al., 2012). These tools are particularly suitable for *transfer zone-crossing* scenarios, which require the extent of the area affected by fault deformation to be determined.

Remote sensing can be used as a starting point for *fault-parallel* and *near-fault tip* scenarios. Unfortunately, the method is limited by the resolution of the data (usually LiDAR with 1 m of resolution is the best available) and the assessment of both damage zone width and displacement can be underestimated, especially for small structures. It can be convenient for non-handy areas and/or in a very initial phase of the study, but the results should be compared with the information reported on official geological cartography and then verified through a fieldwork study.

Remote sensing can also be used to estimate cumulative offset by measuring the height of fault scarps (Haddad et al., 2012) and, for this reason, it can be also useful to perform preliminary hazard assessment in case of *fault-crossing* scenarios. However, considerations derived from remote sensing must be preferably integrated by field observations. Geomorphic methods can be used to estimate throw and slip along faults by studying appropriate landforms that can be directly measured in the field and potentially expanded with aerophotogrammetry (terrestrial LiDAR). When such landforms can be associated with reliable time constraints (e.g. radiometric dating of associated sediments), values can be converted in throw and slip rates (e.g. Nissen et al., 2009). A geological survey with a structural approach allows to enrich the study with surface data and to constrain the fault geometry and kinematics with geological deterministic parameters, especially whether the fault reaches the topographic surface and developed in outcropping rocks. In such a case, a detailed evaluation of the displacement distribution along strike of the main fault surfaces is potentially possible. If the fault remains buried under few meters of recent sediments, on the other hand, it is necessary to find the exact location of the main slip surface(s). In active tectonics studies, geophysical methods offer a useful tool in areas where it may be difficult or even impossible to map/study the surface expression(s) of active faults (for instance in the *near-fault tip* scenario, where faulting may be accommodated by multiple smaller spays that rupture simultaneously during earthquakes), or where information on the subsurface continuation and structure/character of faults is needed. Ground Penetrating Radar (GPR) and Electric Resistivity Tomography (ERT) are also functional to establish the exact point where paleoseismological trenches should be executed. It is important to note that geophysical methods are generally helpful to constrain the vertical component of displacement along faults (not useful for pure strike-slip faults).

The most direct techniques for evaluating the displacement recorded on fault surfaces are paleoseismological studies through trenching and radiometric dating (Galli et al., 2008; McCalpin, 2009; Pantosti et al., 1993). Excavating trenches at specific points across faults, especially in relatively recent sediments, allows for a detailed examination of the stratigraphy of syn-tectonic units, fault-related structures, and displaced geological layers. This can lead to good estimates of the amount of past earthquake-induced fault displacement, recurrence time, slip rates, and magnitude. It should be noted that this would be a punctual value, probably related to the internal and external factors controlling fault propagation up to the ground surface discussed in Sect. 2. For this reason, results may not be representative for the entire ACF but only for the specific analysed fault segment.

Finally, to improve our understanding of faulting within an absolute time frame, specific geochronological constraints are crucial (Hocking et al., 2017; Schimmelpfennig et al., 2009). This can be achieved by direct dating of fault movement represented, for example, by syn-tectonic mineralization (e.g. Uysal et al., 2009; Vignaroli et al., 2022) or exposure of active fault scarps (Benavente et al., 2017; Mozafari et al., 2019).

https://doi.org/10.5194/egusphere-2025-506
Preprint. Discussion started: 4 April 2025

By applying these techniques, we can potentially derive constraints on an average time of recurrence and slip rate (mm/yr) of ACFs, to better evaluate the hazard linked to ground surface displacement.

Table 2: Main interference relationships between ACF and the trace of a linear infrastructure. Direct and indirect methods suitable for their investigation are proposed.

	Crossing		Not crossing	
Interference relationships	***ACF-crossing linear infrastructure***	***Transfer zone-crossing linear infrastructure***	***Near-fault tip linear infrastructure***	***ACF-parallel linear infrastructure***
Main fault aspects to be detailed	Fault displacement recorded on both principal slip surface in the core and subsidiary faults, cumulative offset.	Width of interacting-damage zone, displacement associated with transfer faults if necessary	Width of tip-damage zone	Width of the damage zone. If the linear infrastructure is located out of the damage zone, it is not necessary to proceed with a detailed characterization
Investigations	Structural survey in the field, aerophotogrammetry, geophysical investigations (GPR, ERT), paleoseismological study	Remote Sensing analysis (DTMs, orthophotos, high resolution LiDAR images), aerophotogrammetry, structural survey in the field, paleoseismological study	Remote Sensing analysis (DTMs, high resolution LiDAR images), aerophotogrammetry, structural survey in the field, geophysical investigations (GPR, ERT)	Remote Sensing analysis (DTMs, orthophotos, high resolution LiDAR images), aerophotogrammetry, structural survey in the field

6 Conclusions

ACFs characterization is becoming of increasing importance to seismic hazard assessment during the planning of linear infrastructures, as they can produce permanent deformation of the ground surface. Thus, the feasibility phase of a new linear infrastructure should carefully consider the structural study of these complex tectonic structures, which are very common in tectonically active regions, such as most of the Italian territory. This impact can result from a number of factors related to the structural complexity of the internal architecture of the ACFs, which includes fault core, wall-damage zone, tip-damage zone and transfer zones between two or more faults (or fault segments). As these aspects vary significantly along and across strike of a fault system, it follows that fault-related hazard can vary and, in certain cases, be related more to a specific parameter than others. Consequently, the hazard value also depends on the portion of the fault zone being crossed by the planned linear infrastructure. We distinguished four possible interference relations between the planned infrastructure line and an ACF. For each case, we determined: a) the main fault structural aspects to be detected with higher priority; b) which parameters weigh more in the hazard evaluation; c) the most suitable investigations to employ, considering that the geological and structural study in the field remains a fundamental step. This is expected to provide a new structural geology-based methodological approach for the hazard assessment related to ACFs, which can support infrastructural planning in the preliminary stages of a feasibility project study. This approach is compatible with the timing and budget requirements associated with design projects, and, at the same time, appears to be more detailed and complete than conventional seismic hazard assessment methods, since it considers with increased resolution the structural complexity of fault zones. Furthermore, predicting a certain level of seismic hazard along the linear infrastructure represents a key step in planning, which contributes to improved resilience of the infrastructure itself.

https://doi.org/10.5194/egusphere-2025-506
Preprint. Discussion started: 4 April 2025

Author contribution

Selina Bonini: Conceptualization, Investigation, Writing – original draft preparation, reviewing & editing, Validation, Visualization, Methodology. *Riccardo Asti*: Writing – reviewing & editing, investigation, Supervision. *Giulio Viola*: Supervision, Writing – review & editing, Validation, Funding acquisition. *Giulia Tartaglia*: Writing – reviewing & editing, Validation, Supervision. *Stefano Rodani*: Validation, Supervision. *Gianluca Benedetti*: Validation, Supervision. *Massimo Comedini*: Validation, Supervision, Funding acquisition. *Gianluca Vignaroli*: Conceptualization, Project administration, Validation, Supervision, Writing – review & editing, Funding acquisition.

Competing interests

The authors declare that they have no conflict of interest.

ACKNOWLEDGEMENTS

This work belongs to the PhD project of S. Bonini "Parameters for assessing active faulting and related surface effects in railway design". The project is funded by a research agreement between ITALFERR S.p.A. and BiGeA Dept (CONTRATTO PER IL COFINANZIAMENTO DI BORSE DI DOTTORATO ATTIVATE AI SENSI DEL DM 352 DEL 9 APRILE 2022 - 38° CICLO - A.A. 2022/2023). This work is also partially supported by the PE3 RETURN Project (CUP J33C22002840002; R.A. and G. Vignaroli).

References

Acocella, V., Gudmundsson, A., and Funiciello, R.: Interaction and linkage of extension fractures and normal faults: examples from the rift zone of Iceland, J Struct Geol, 22, 1233–1246, 2000.

An, L.-J.: Maximum link distance between strike-slip faults: observations and constraints, Pure Appl Geophys, 150, 19–36, 1997.

Axen, G. J., Fletcher, J. M., Cowgill, E., Murphy, M., Kapp, P., MacMillan, I., Ramos-Velàzquez, E., and Aranda-Gomez, J.: Range-front fault scarps of the Sierra El Mayor, Baja California: Formed above an active low-angle normal fault?, Geology, 27, 247–250, 1999.

Barnett, J. A. M., Mortimer, J., Rippon, J. J., Walsh, J. J., and Watterson, J.: Displacement Geometry in the Volume Containing a Single Normal Fault, The American Association of Petroleum Geologist Bulletin, 71, 925–937, 1987.

Bastesen, E. and Braathen, A.: Extensional faults in fine grained carbonates – analysis of fault core lithology and thickness–displacement relationships, J Struct Geol, 32, 1609–1628, https://doi.org/10.1016/J.JSG.2010.09.008, 2010.

Benavente, C., Zerathe, S., Audin, L., Hall, S. R., Robert, X., Delgado, F., Carcaillet, J., and Team, A.: Active transpressional tectonics in the Andean forearc of southern Peru quantified by ^{10}Be surface exposure dating of an active fault scarp, Tectonics, 36, 1662–1678, https://doi.org/10.1002/2017TC004523, 2017.

Ben-Zion, Y. and Sammis, C. G.: Characterization of Fault Zones, Pure Appl Geophys, 160, 677–715, https://doi.org/10.1007/PL00012554, 2003.

Berg, S. S. and Skar, T.: Controls on damage zone asymmetry of a normal fault zone: outcrop analyses of a segment of the Moab fault, SE Utah, J Struct Geol, 27, 1803–1822, https://doi.org/10.1016/j.jsg.2005.04.012, 2005.

Billi, A., Salvini, F., and Storti, F.: The damage zone-fault core transition in carbonate rocks: implications for fault growth, structure and permeability, J Struct Geol, 25, 1779–1794, https://doi.org/10.1016/S0191-8141(03)00037-3, 2003.

https://doi.org/10.5194/egusphere-2025-506
Preprint. Discussion started: 4 April 2025

Bott, M. H. P.: The Mechanics of Oblique Slip Faulting, Geol Mag, 96, 109–117, https://doi.org/10.1017/S0016756800059987, 1959.

Bray, J. D., Seed, R. B., Cluff, L. S., and Seed, H. B.: Earthquake Fault Rupture Propagation through Soil, Journal of Geotechnical Engineering, 120, 543–561, https://doi.org/10.1061/(ASCE)0733-9410(1994)120:3(543), 1994.

Bruhn, R. L., Parry, W. T., Yonkee, W. A., and Thompson, T.: Fracturing and hydrothermal alteration in normal fault zones, Pure Appl Geophys, 142, 609–644, https://doi.org/10.1007/BF00876057, 1994.

Caine, J. S., Evans, J. P., and Forster, C. B.: Fault zone architecture and permeability structure, Geology, 24, 1025–1028, 1996.

Cartwright, J. A., Trudgill, B. D., and Mansfield, C. S.: Fault growth by segment linkage: an explanation for scatter in maximum displacement and trace length data from the Canyonlands Grabens of SE Utah, J Struct Geol, 17, 1319–1326, https://doi.org/10.1016/0191-8141(95)00033-A, 1995.

Cello, G., Deiana, G., Ferelli, L., Marchegiani, L., Maschio, L., Mazzoli, S., Michetti, A., Serva, L., Tondi, E., and Vittori, T.: Geological constraints for earthquake faulting studies in the Colfiorito area (central Italy), J Seismol, 4, 357–364, https://doi.org/10.1023/A:1026525302837, 2000.

Chester, F. M. and Logan, J. M.: Implications for mechanical properties of brittle faults from observations of the Punchbowl fault zone, California, Pure Appl Geophys, 124, 79–106, https://doi.org/10.1007/BF00875720, 1986.

Chester, F. M. and Logan, J. M.: Composite planar fabric of gouge from the Punchbowl Fault, California, J Struct Geol, 9, 621-IN6, https://doi.org/10.1016/0191-8141(87)90147-7, 1987.

Chester, F. M., Evans, J. P., and Biegel, R. L.: Internal structure and weakening mechanisms of the San Andreas Fault, J Geophys Res Solid Earth, 98, 771–786, https://doi.org/10.1029/92JB01866, 1993.

Childs, C., Nicol, A., Walsh, J. J., and Watterson, J.: Growth of vertically segmented normal faults, J Struct Geol, 18, 1389–1397, https://doi.org/10.1016/S0191-8141(96)00060-0, 1996.

Childs, C., Manzocchi, T., Walsh, J. J., Bonson, C. G., Nicol, A., and Schöpfer, M. P. J.: A geometric model of fault zone and fault rock thickness variations, J Struct Geol, 31, 117–127, https://doi.org/10.1016/j.jsg.2008.08.009, 2009.

Clark, D. J., Brennand, S., Brenn, G., Garthwaite, M. C., Dimech, J., Allen, T. I., and Standen, S.: Surface deformation relating to the 2018 Lake Muir earthquake sequence, southwest Western Australia: new insight into stable continental region earthquakes, Solid Earth, 11, 691–717, https://doi.org/10.5194/se-11-691-2020, 2020.

Cowie, P. A. and Roberts, G. P.: Constraining slip rates and spacings for active normal faults, J Struct Geol, 23, 1901–1915, https://doi.org/10.1016/S0191-8141(01)00036-0, 2001.

Cowie, P. A. and Shipton, Z. K.: Fault tip displacement gradients and process zone dimensions, J Struct Geol, 20, 983–997, https://doi.org/10.1016/S0191-8141(98)00029-7, 1998.

Cox, S. J. D. and Scholz, C. H.: On the formation and growth of faults: an experimental study, J Struct Geol, 10, 413–430, https://doi.org/10.1016/0191-8141(88)90019-3, 1988.

Dai, X., Liu, X., Liu, R., Song, M., Zhu, G., Chang, X., and Guo, J.: Coseismic Slip Distribution and Coulomb Stress Change of the 2023 MW 7.8 Pazarcik and MW 7.5 Elbistan Earthquakes in Turkey, Remote Sens (Basel), 16, 240, https://doi.org/10.3390/rs16020240, 2024.

Evans, J. P.: Thickness-displacement relationships for fault zones, J Struct Geol, 12, 1061–1065, https://doi.org/10.1016/0191-8141(90)90101-4, 1990.

Faulkner, D. R., Lewis, A. C., and Rutter, E. H.: On the internal structure and mechanics of large strike-slip fault zones: field observations of the Carboneras fault in southeastern Spain, Tectonophysics, 367, 235–251, https://doi.org/10.1016/S0040-1951(03)00134-3, 2003.

https://doi.org/10.5194/egusphere-2025-506
Preprint. Discussion started: 4 April 2025

Faulkner, D. R., Mitchell, T. M., Rutter, E. H., and Cembrano, J.: On the structure and mechanical properties of large strike-slip faults, Geological Society, London, Special Publications, 299, 139–150, https://doi.org/10.1144/SP299.9, 2008.

Faulkner, D. R., Jackson, C. A. L., Lunn, R. J., Schlische, R. W., Shipton, Z. K., Wibberley, C. A. J., and Withjack, M. O.: A review of recent developments concerning the structure, mechanics and fluid flow properties of fault zones, J Struct Geol, 32, 1557–1575, https://doi.org/10.1016/j.jsg.2010.06.009, 2010.

Faulkner, D. R., Mitchell, T. M., Jensen, E., and Cembrano, J.: Scaling of fault damage zones with displacement and the implications for fault growth processes, J Geophys Res Solid Earth, 116, https://doi.org/10.1029/2010JB007788, 2011.

Ferrill, D. A., Morris, A. P., Sims, D. W., Waiting, D. J., and Hasegawa, S.: Development of synthetic layer dip adjacent to normal faults, American Association of Petroleum Geologists Memoir, 85, 125–138, 2005.

Ferrill, D. A., Smart, K. J., and Necsoiu, M.: Displacement-length scaling for single-event fault ruptures: insights from Newberry Springs Fault Zone and implications for fault zone structure, Geological Society, London, Special Publications, 299, 113–122, https://doi.org/10.1144/SP299.7, 2008.

Fletcher, J. M. and Spelz, R. M.: Patterns of Quaternary deformation and rupture propagation associated with an active low-angle normal fault, Laguna Salada, Mexico: Evidence of a rolling hinge?, Geosphere, 5, 385–407, https://doi.org/10.1130/GES00206.1, 2009.

Fossen, H. and Rotevatn, A.: Fault linkage and relay structures in extensional settings—A review, Earth Sci Rev, 154, 14–28, https://doi.org/10.1016/j.earscirev.2015.11.014, 2016.

Fossen, H., Schulz, R. A., Shipton, Z. K., and Mair, K.: Deformation bands in sandstone, a review, Journal of Geological Society of London, 164, 755–769, 2007.

Foxford, K. A., Walsh, J. J., Watterson, J., Garden, I. R., Guscott, S. C., and Burley, S. D.: Structure and content of the Moab Fault Zone, Utah, USA, and its implications for fault seal prediction, Geological Society, London, Special Publications, 147, 87–103, https://doi.org/10.1144/GSL.SP.1998.147.01.06, 1998.

Fujii, Y., Satake, K., Watada, S., and Ho, T.-C.: Re-examination of Slip Distribution of the 2004 Sumatra–Andaman Earthquake (Mw 9.2) by the Inversion of Tsunami Data Using Green's Functions Corrected for Compressible Seawater Over the Elastic Earth, Pure Appl Geophys, 178, 4777–4796, https://doi.org/10.1007/s00024-021-02909-6, 2021.

Galadini, F. and Galli, P.: The Holocene paleoearthquakes on the 1915 Avezzano earthquake faults (central Italy): implications for active tectonics in the central Apennines, Tectonophysics, 308, 143–170, https://doi.org/10.1016/S0040-1951(99)00091-8, 1999.

Galli, P., Galadini, F., and Pantosti, D.: Twenty years of paleoseismology in Italy, Earth Sci Rev, 88, 89–117, https://doi.org/10.1016/j.earscirev.2008.01.001, 2008.

Giba, M., Walsh, J. J., and Nicol, A.: Segmentation and growth of an obliquely reactivated normal fault, J Struct Geol, 39, 253–267, https://doi.org/10.1016/j.jsg.2012.01.004, 2012.

Goddard, J. V. and Evans, J. P.: Chemical changes and fluid-rock interaction in faults of crystalline thrust sheets, northwestern Wyoming, U.S.A., J Struct Geol, 17, 533–547, https://doi.org/10.1016/0191-8141(94)00068-B, 1995.

Haddad, D. E., Akciz, S. O., Arrowsmith, J. R., Rhodes, D. D., Oldow, J. S., Zielke, O., Toke, N. A., Haddad, A. G., Mauer, J., and Shilpakar, P.: Applications of airborne and terrestrial laser scanning to paleoseismology, Geosphere, 8, 771–786, https://doi.org/10.1130/GES00701.1, 2012.

Hocking, E. P., Garrett, E., and Cisternas, M.: Modern diatom assemblages from Chilean tidal marshes and their application for quantifying deformation during past great earthquakes, J Quat Sci, 32, 396–415, https://doi.org/10.1002/jqs.2933, 2017.

Horsfield, W. T.: An experimental approach to basement-controlled faulting, Geologie en Mijbouw, 56, 1977.

https://doi.org/10.5194/egusphere-2025-506
Preprint. Discussion started: 4 April 2025

Huang, W. and Johnson, A. M.: Quantitative description and analysis of earthquake-induced deformation zones along strike-slip and dip-slip faults, J Geophys Res Solid Earth, 115, https://doi.org/10.1029/2009JB006361, 2010.

International Atomic Energy Agency: Seismic Hazards in Site Evaluation for Nuclear Installations. Specific Safety Guide No. SSG-9, Vienna, 2010.

Irvine, P. J. and Hill, R. L.: Surface rupture along a portion of the Emerson fault, Landers earthquake of June 28, 1992. California, Geology, 46, 23–26, 1993.

ITHACA (ITaly HAzard from CApable faulting), A database of active capable faults of the Italian territory: http://sgi2.isprambiente.it/ithacaweb/Mappatura.aspx, last access: 9 October 2024.

Johannessen, M. U.: Fault core and its geostatistical analysis: Insight into the fault core thickness and fault displacement, Thesis for Master's degree, University of Bergen, 2017.

Johnson, A. M., Fleming, R. W., Cruikshank, K. M., Martosudarmo, S. Y., Johnson, N. A., Johnson, K. M., and Wei, W.: Analecta of structures formed during the 28 June 1992 Landers-Big Bear, California, earthquake sequence, 94–97 pp., 1997.

Kim, Y. S. and Sanderson, D. J.: The relationship between displacement and length of faults: A review, Earth Sci Rev, 68, 317–334, https://doi.org/10.1016/j.earscirev.2004.06.003, 2005.

Kim, Y. S. and Sanderson, D. J.: Structural similarity and variety at the tips in a wide range of strike-slip faults: A review, Terra Nova, 18, 330–344, https://doi.org/10.1111/j.1365-3121.2006.00697.x, 2006.

Kim, Y. S., Peacock, D. C. P., and Sanderson, D. J.: Fault damage zones, J Struct Geol, 26, 503–517, https://doi.org/10.1016/j.jsg.2003.08.002, 2004.

Kim, Y.-S., Andrews, J. R., and Sanderson, D. J.: Damage zones around strike-slip fault systems and strike-slip fault evolution, Crackington Haven, southwest England, Geosciences Journal, 4, 53–72, https://doi.org/10.1007/BF02910127, 2000.

Kim, Y.-S., Peacock, D. C. P., and Sanderson, D. J.: Mesoscale strike-slip faults and damage zones at Marsalforn, Gozo Island, Malta, J Struct Geol, 25, 793–812, https://doi.org/10.1016/S0191-8141(02)00200-6, 2003.

Klinger, Y., Xu, X., Tapponnier, P., Van Der Woerd, J., Lasserre, C., and King, G.: High-Resolution Satellite Imagery Mapping of the Surface Rupture and Slip Distribution of the Mw 7.8, 14 November 2001 Kokoxili Earthquake, Kunlun Fault, Northern Tibet, China, Bulletin of the Seismological Society of America, 95, 1970–1987, https://doi.org/10.1785/0120040233, 2005.

Lasserre, C., Peltzer, G., Crampé, F., Klinger, Y., Van der Woerd, J., and Tapponnier, P.: Coseismic deformation of the 2001 Mw = 7.8 Kokoxili earthquake in Tibet, measured by synthetic aperture radar interferometry, J Geophys Res Solid Earth, 110, https://doi.org/10.1029/2004JB003500, 2005.

Lazarte, C. A., Bray, J. D., Johnson, A. M., and Lemmer, R. E.: Surface breakage of the 1992 Landers earthquake and its effects on structures, Bulletin of the Seismological Society of America, 84, 547–561, https://doi.org/10.1785/BSSA0840030547, 1994.

Leonard, M.: Earthquake fault scaling: Self-consistent relating of rupture length, width, average displacement, and moment release, Bulletin of the Seismological Society of America, 100, 1971–1988, https://doi.org/10.1785/0120090189, 2010.

Lienkaemper, J. J., Baker, B., and McFarland, F. S.: Surface Slip Associated with the 2004 Parkfield, California, Earthquake Measured on Alinement Arrays, Bulletin of the Seismological Society of America, 96, S239–S249, https://doi.org/10.1785/0120050806, 2006.

https://doi.org/10.5194/egusphere-2025-506
Preprint. Discussion started: 4 April 2025

Ma, S.: Distinct asymmetry in rupture-induced inelastic strain across dipping faults: An off-fault yielding model, Geophys Res Lett, 36, https://doi.org/10.1029/2009GL040666, 2009.

McCalpin, J. P.: Paleoseismology, 2nd ed., 2009.

McCalpin, J. P.: Statistic of paleoseismic data. Program Element III: Understanding earthquake processes, 2013.

McGrath, A. G. and Davison, I.: Damage zone geometry around fault tips, J Struct Geol, 17, 1011–1024, 1995.

Melissianos, V. E., Danciu, L., Vamvatsikos, D., and Basili, R.: Fault displacement hazard estimation at lifeline–fault crossings: A simplified approach for engineering applications, Bulletin of Earthquake Engineering, 21, 4821–4849, https://doi.org/10.1007/s10518-023-01710-1, 2023.

Morley, C. K., Nelson, R. A., Patton, T. L., and Munn, S. G.: Transfer Zones in the East African Rift System and Their Relevance to Hydrocarbon Exploration in Rifts (1), The American Association of Petroleum Geologists Bulletin, 74, 1234–1253, https://doi.org/10.1306/0C9B2475-1710-11D7-8645000102C1865D, 1990.

Moss, R. E. S. and Ross, Z. E.: Probabilistic Fault Displacement Hazard Analysis for Reverse Faults, Bulletin of the Seismological Society of America, 101, 1542–1553, https://doi.org/10.1785/0120100248, 2011.

Mozafari, N., Tikhomirov, D., Sumer, Ö., Özkaymak, Ç., Uzel, B., Yeşilyurt, S., Ivy-Ochs, S., Vockenhuber, C., Sözbilir, H., and Akçar, N.: Dating of active normal fault scarps in the Büyük Menderes Graben (western Anatolia) and its implications for seismic history, Quat Sci Rev, 220, 111–123, https://doi.org/10.1016/j.quascirev.2019.07.002, 2019.

Naylor, M. A., Mandl, G., and Supesteijn, C. H. K.: Fault geometries in basement-induced wrench faulting under different initial stress states, J Struct Geol, 8, 737–752, https://doi.org/10.1016/0191-8141(86)90022-2, 1986.

Nissen, E., Walker, R., Molor, E., Fattahi, M., and Bayasgalan, A.: Late Quaternary rates of uplift and shortening at Baatar Hyarhan (Mongolian Altai) with optically stimulated luminescence, Geophys J Int, 177, 259–278, https://doi.org/10.1111/j.1365-246X.2008.04067.x, 2009.

Nissen, E., Krishnan, A. K., Arrowsmith, J. R., and Saripalli, S.: Three-dimensional surface displacements and rotations from differencing pre- and post-earthquake LiDAR point clouds, Geophys Res Lett, 39, https://doi.org/10.1029/2012GL052460, 2012.

Nurminen, F., Baize, S., Boncio, P., Blumetti, A. M., Cinti, F. R., Civico, R., and Guerrieri, L.: SURE 2.0 – New release of the worldwide database of surface ruptures for fault displacement hazard analyses, Sci Data, 9, 729, https://doi.org/10.1038/s41597-022-01835-z, 2022.

Odling, N. E., Harris, S. D., and Knipe, R. J.: Permeability scaling properties of fault damage zones in siliclastic rocks, J Struct Geol, 26, 1727–1747, https://doi.org/10.1016/j.jsg.2004.02.005, 2004.

Pantosti, D., Schwartz, D. P., and Valensise, G.: Paleoseismology along the 1980 surface rupture of the Irpinia Fault: Implications for earthquake recurrence in the southern Apennines, Italy, J Geophys Res Solid Earth, 98, 6561–6577, https://doi.org/10.1029/92JB02277, 1993.

Peacock, D. C. P.: Propagation, interaction and linkage in normal fault systems, Earth Sci Rev, 58, 121–142, https://doi.org/10.1016/S0012-8252(01)00085-X, 2002.

Peacock, D. C. P. and Sanderson, D. J.: Displacements, segment linkage and relay ramps in normal fault zones, J Struct Geol, 13, 721–733, https://doi.org/10.1016/0191-8141(91)90033-F, 1991.

Peacock, D. C. P. and Sanderson, D. J.: Geometry and Development of Relay Ramps in Normal Fault Systems, The American Association of Petroleum Geologists Bulletin, 78, 147–165, https://doi.org/10.1306/BDFF9046-1718-11D7-8645000102C1865D, 1994.

Peacock, D. C. P., Dimmen, V., Rotevatn, A., and Sanderson, D. J.: A broader classification of damage zones, J Struct Geol, 102, 179–192, https://doi.org/10.1016/j.jsg.2017.08.004, 2017.

https://doi.org/10.5194/egusphere-2025-506
Preprint. Discussion started: 4 April 2025

Petersen, M. D., Dawson, T. E., Chen, R., Cao, T., Wills, C. J., Schwartz, D. P., and Frankel, A. D.: Fault Displacement Hazard for Strike-Slip Faults, Bulletin of the Seismological Society of America, 101, 805–825, https://doi.org/10.1785/0120100035, 2011.

Philip, H., Rogozhin, E., Cisternas, A., Bousquet, J. C., Borisov, B., and Karakhanian, A.: The Armenian earthquake of 1988 December 7: faulting and folding, neotectonics and palaeoseismicity, Geophys J Int, 110, 141–158, https://doi.org/10.1111/j.1365-246X.1992.tb00718.x, 1992.

Prentice, C. S. and Ponti, D. J.: Coseismic deformation of the Wrights tunnel during the 1906 San Francisco earthquake: A key to understanding 1906 fault slip and 1989 surface ruptures in the southern Santa Cruz Mountains, California, J Geophys Res Solid Earth, 102, 635–648, https://doi.org/10.1029/96jb02934, 1997.

Quigley, M., Van Dissen, R., Litchfield, N., Villamor, P., Duffy, B., Barrell, D., Furlong, K., Stahl, T., Bilderback, E., and Noble, D.: Surface rupture during the 2010 Mw 7.1 Darfield (Canterbury) earthquake: Implications for fault rupture dynamics and seismic-hazard analysis, Geology, 40, 55–58, https://doi.org/10.1130/G32528.1, 2012.

Reid, H. F.: Report of the State Earthquake Investigation Commission, II: The mechanics of the earthquake, Washington, D.C., 1910.

Ritz, J.-F., Baize, S., Ferry, M., Larroque, C., Audin, L., Delouis, B., and Mathot, E.: Surface rupture and shallow fault reactivation during the 2019 Mw 4.9 Le Teil earthquake, France, Commun Earth Environ, 1, 10, https://doi.org/10.1038/s43247-020-0012-z, 2020.

Schimmelpfennig, I., Benedetti, L., Finkel, R., Pik, R., Blard, P.-H., Bourlès, D., Burnard, P., and Williams, A.: Sources of in-situ 36Cl in basaltic rocks. Implications for calibration of production rates, Quat Geochronol, 4, 441–461, https://doi.org/10.1016/j.quageo.2009.06.003, 2009.

Schlische, R. W., Withjack, M. O., and Eisenstadt, G.: An experimental study of the secondary deformation produced by oblique-slip normal faulting, The American Association of Petroleum Geologists Bulletin, 86, 885–906, https://doi.org/10.1306/61EEDBCA-173E-11D7-8645000102C1865D, 2002.

Scholz, C. H.: Permeability of faults, in: The Mechanical iIvolvement of Fluids in Faulting, edited by: Hickman, S., Bruhn, R. L., and Sibson, R., U.S. Geological Survey Open-File Report 94 - 228, 132–137, 1994.

Schultz, R. A.: Understanding the process of faulting: selected challenges and opportunities at the edge of the 21st century, J Struct Geol, 21, 985–993, https://doi.org/10.1016/S0191-8141(99)00025-5, 1999.

Schultz, R. A., Soliva, R., Fossen, H., Okubo, C. H., and Reeves, D. M.: Dependence of displacement–length scaling relations for fractures and deformation bands on the volumetric changes across them, J Struct Geol, 30, 1405–1411, https://doi.org/10.1016/j.jsg.2008.08.001, 2008.

Shinoda, M., Yoshida, I., Watanabe, K., Nakajima, S., Nakamura, S., and Miyata, Y.: Seismic probabilistic risk estimation of Japanese railway embankments and risk-based design strength of soil and reinforcement, Soil Dynamics and Earthquake Engineering, 163, 107507, https://doi.org/10.1016/j.soildyn.2022.107507, 2022.

Shipton, Z., Evans, J., and Thompson, L.: The geometry and thickness of deformation-band fault core and its influence on sealing characteristics of deformation-band fault zones, The American Association of Petroleum Geologists Memoir, 85, 181–195, 2005.

Shipton, Z. K., Soden, A. M., Kirkpatrick, J. D., Bright, A. M., and Lunn, R. J.: How thick is a fault? Fault displacement-thickness scaling revisited, 193–198, https://doi.org/10.1029/170GM19, 2006.

Sibson, R. H.: Fault rocks and fault mechanisms, J Geol Soc London, 133, 191–213, https://doi.org/10.1144/gsjgs.133.3.0191, 1977.

https://doi.org/10.5194/egusphere-2025-506
Preprint. Discussion started: 4 April 2025

Smith, L., Foster, C. B., and Evans, J. P.: Interaction Between Fault Zones, Fluid Flow and Heat Transfer at the Basin Scale, in: Hydrogeology of Low Permeability Environments, vol. 2, edited by: Newman, S. P. and Neretnieks, I., International Association of Hydrological Sciences selected papers in Hydrogeology, 41–67, 1990.

Sperrevik, S., Gillespie, P. A., Fisher, Q. J., Halvorsen, T., and Knipe, R. J.: Empirical estimation of fault rock properties, Norwegian Petroleum Society Special Publications , 11, 109–125, 2002.

Tchalenko, J. S.: Similarities between shear zones of different magnitudes, Geol Soc Am Bull, 81, 1625–1640, 1970.

Technical Commission on Seismic Microzonation: Land use guidelines for areas with active and capable faults (ACF), Conference of the Italian Regions and Autonomous Provinces - Rome, 2015.

Torabi, A. and Berg, S. S.: Scaling of fault attributes: A review, Mar Pet Geol, 28, 1444–1460, 2011.

Torabi, A., Johannessen, M. U., and Ellingsen, T. S. S.: Fault Core Thickness: Insights from Siliciclastic and Carbonate Rocks, Geofluids, 2019, 1–24, https://doi.org/10.1155/2019/2918673, 2019.

Torabi, A., Ellingsen, T. S. S., Johannessen, M. U., Alaei, B., Rotevatn, A., and Chiarella, D.: Fault zone architecture and its scaling laws: where does the damage zone start and stop?, Geological Society, London, Special Publications, 496, 99–124, https://doi.org/10.1144/SP496-2018-151, 2020.

Treiman, J. A.: Fault Rupture and Surface Deformation: Defining the Hazard, Environmental and Engineering Geoscience, 16, 19–30, https://doi.org/10.2113/gseegeosci.16.1.19, 2010.

Trudgill, B. and Cartwright, J.: Relay-ramp forms and normal-fault linkages, Canyonlands National Park, Utah, Geol Soc Am Bull, 106, 1143–1157, 1994.

Uysal, I. T., Feng, Y., Zhao, J., Isik, V., Nuriel, P., and Golding, S. D.: Hydrothermal CO2 degassing in seismically active zones during the late Quaternary, Chem Geol, 265, 442–454, https://doi.org/10.1016/j.chemgeo.2009.05.011, 2009.

Vermilye, J. M. and Scholz, C. H.: The process zone: A microstructural view of fault growth, J Geophys Res Solid Earth, 103, 12223–12237, https://doi.org/10.1029/98JB00957, 1998.

Vignaroli, G., Rossetti, F., Petracchini, L., Argante, V., Bernasconi, S. M., Brilli, M., Giustini, F., Yu, T.-L., Shen, C.-C., and Soligo, M.: Middle Pleistocene fluid infiltration with 10–15 ka recurrence within the seismic cycle of the active Monte Morrone Fault System (central Apennines, Italy), Tectonophysics, 827, 229269, https://doi.org/10.1016/j.tecto.2022.229269, 2022.

Wallace, R. E.: Geometry of Shearing Stress and Relation to Faulting, J Geol, 59, 118–130, https://doi.org/10.1086/625831, 1951.

Walsh, J. J., Nicol, A., and Childs, C.: An alternative model for the growth of faults, J Struct Geol, 24, 1669–1675, https://doi.org/10.1016/S0191-8141(01)00165-1, 2002.

Walsh, J. J., Bailey, W. R., Childs, C., Nicol, A., and Bonson, C. G.: Formation of segmented normal faults: a 3-D perspective, J Struct Geol, 25, 1251–1262, https://doi.org/10.1016/S0191-8141(02)00161-X, 2003.

Wells, D. L. and Coppersmith, K. J.: New empirical relationships among magnitude, rupture length, rupture width, rupture area, and surface displacement, Bulletin of the Seismological Society of America, 84, 974–1002, https://doi.org/10.1785/BSSA0840040974, 1994.

Wesnousky, S. G.: Displacement and geometrical characteristics of earthquake surface ruptures: Issues and implications for seismic-hazard analysis and the process of earthquake rupture, Bulletin of the Seismological Society of America, 98, 1609–1632, https://doi.org/10.1785/0120070111, 2008.

Wibberley, C. A., Yielding, G., and Di Toro, G.: Recent advances in the understanding of fault zone internal structure: a review, Journal of Geological Society of London, Special Publications, 299, 5–33, 2008.

https://doi.org/10.5194/egusphere-2025-506
Preprint. Discussion started: 4 April 2025

Youd, T. L.: Ground failure investigations following the 1964 Alaska earthquake, in: NCEE 2014 - 10th U.S. National Conference on Earthquake Engineering: Frontiers of Earthquake Engineering, https://doi.org/10.4231/D3DN3ZW6P, 2014.

Youngs, R. R., Arabasz, W. J., Anderson, R. E., Ramelli, A. R., Ake, J. P., Slemmons, D. B., McCalpin, J. P., Doser, D. I., Fridrich, C. J., Swan, F. H., Rogers, A. M., Yount, J. C., Anderson, L. W., Smith, K. D., Bruhn, R. L., Knuepfer, P. L. K., Smith, R. B., DePolo, C. M., O'Leary, D. W., Coppersmith, K. J., Pezzopane, S. K., Schwartz, D. P., Whitney, J. W., Olig, S. S., and Toro, G. R.: A methodology for probabilistic fault displacement hazard analysis (PFDHA), Earthquake Spectra, 19, 191–219, https://doi.org/10.1193/1.1542891, 2003.

van der Zee, W. and Urai, J. L.: Processes of normal fault evolution in a siliciclastic sequence: a case study from Miri, Sarawak, Malaysia, J Struct Geol, 27, 2281–2300, 2005.

Zhu, W., Liu, K., Wang, M., and Koks, E. E.: Seismic Risk Assessment of the Railway Network of China's Mainland, International Journal of Disaster Risk Science, 11, 452–465, https://doi.org/10.1007/s13753-020-00292-9, 2020.